

Compact stars with a quark core within NJL model

C. H. Lenzi^{1,2}, A. S. Schneider³, C. Providência², R. M. Marinho Jr.¹

¹*Departamento de Física, Instituto Tecnológico de Aeronáutica,
Campo Montenegro, São José dos Campos, SP, 12228-900, Brazil*

²*Centro de Física Computacional, Department of Physics,
University of Coimbra, Rua Larga, Coimbra, 3004-516, Portugal*

³*Department of Physics, Indiana University, Swain Hall West 117,
727 East Third Street Bloomington, Indiana 47405*

(Dated: January 18, 2010)

An ultraviolet cutoff dependent on the chemical potential as proposed by Casalbuoni *et al* is used in the su(3) Nambu-Jona-Lasinio model. The model is applied to the description of stellar quark matter and compact stars. It is shown that with a new cutoff parametrization it is possible to obtain stable hybrid stars with a quark core. A larger cutoff at finite densities leads to a partial chiral symmetry restoration of quark s at lower densities. A direct consequence is the onset of the s quark in stellar matter at lower densities and a softening of the equation of state.

PACS numbers:

I. INTRODUCTION

Compact stars are complex systems which may contain exotic matter such as hyperons, kaon condensation, a non-homogenous mixed quark-hadron phase or, in their core, a pure quark phase [1, 2].

The hadronic phase has been successfully described within a relativistic mean-field theory with the inclusion of hyperons (for a review see [1]). The quark phase has frequently been described by the schematic MIT bag model [3, 4] or by the Nambu-Jona-Lasinio (NJL) model [5, 6]. The NJL model contains some of the basic symmetries of QCD, namely chiral symmetry. It has been very successful in describing the vacuum properties of low lying mesons and predicts at sufficiently high densities/temperatures a phase transition to a chiral symmetric state [7–10]. However, it is just an effective theory that does not take into account quark confinement.

The authors of [11] have studied the possible existence of deconfined quark matter in the interior of neutron stars using the NJL model to describe the quark phase and could show that within this model typical neutron stars do not possess any deconfined quark matter in their center. It was shown that as soon as quark matter appears the star becomes unstable and collapses into a black-hole. It was also pointed out that the large constituent strange quark mass obtained with NJL over a wide range of densities was the cause of this behavior. In [12] it was shown that for warm neutrino free stellar matter a small quark core could appear at finite temperature. The reason can be traced back to a faster reduction of the s quark constituent mass at low densities and, therefore, the onset of the s quark at lower densities. For warm stellar matter with an entropy per particle equal or below 2, with or without trapped neutrinos no quark core was obtained [13].

Over the last decade, it has been realized that strong interacting matter at high density and low temperature may possess a large assortment of phases. Different pos-

sible patterns for color superconductivity [14] have been conjectured (for a review see *e.g.* [15, 16] and references therein quoted). Very recently, a new phase of QCD, named quarkyonic phase, characterized by chiral symmetry and confinement has been predicted [17]. We will not consider these phases in the present work.

It was shown in [18] that at very large densities the standard NJL model is not able to reproduce the correct QCD behavior of the gap parameter in the quark color flavor locked (CFL) phase. In order to solve this problem Casalbuoni *et al* have introduced a ultraviolet cutoff dependent on the baryonic chemical potential [18]. The dependence of a parameter of the model on the chemical potential changes the thermodynamics of the model and has to be dealt with care [19]. Within su(2) NJL Baldo *et al* have investigated whether a cutoff dependent on the chemical potential could solve the problem of star instability with the onset of the quark phase and concluded that this was not a solution [20]. The question that may be raised is whether within the su(3) NJL a different behavior occurs due to the a different behavior of the s quark constituent mass with density. We will show that a larger cutoff at finite baryonic densities will move the onset of the s quark to smaller densities due to a faster decrease of the s quark constituent mass with density.

After a review of the standard su(3) NJL model we will introduce in section II the parametrization of the cutoff dependence on the chemical potential, the thermodynamic consistency of the modified model and the β -equilibrium conditions. In section III we discuss the star stability and the dependence of the maximum mass configuration on the cutoff. In the last section we draw some conclusions.

II. THE MODIFIED SU(3) NAMBU-JONA-LASINIO MODEL

A. Standard su(3) NJL model

To describe quark matter phase in neutron star, we use the su(3) NJL model with scalar-pseudoscalar and 't Hooft six fermion interaction. The Lagrangian density of NJL model is defined by [12]:

$$\mathcal{L} = \bar{\psi} (i\gamma^\mu \partial_\mu + \hat{m}_0) \psi + g_s \sum_{a=0}^8 \left[(\bar{\psi} \lambda^a \psi)^2 + (\bar{\psi} i\gamma_5 \lambda^a \psi)^2 \right] + g_t \{ \det [\bar{\psi}_i (1 + \gamma_5) \psi_j] + \det [\bar{\psi}_i (1 - \gamma_5) \psi_j] \}, \quad (1)$$

where, in flavor space, $\psi = (u; d; s)$ denotes the quark fields and the λ^a matrices are generators of the u(3) algebra. The term $\hat{m}_0 = \text{diag}(m_{0u}, m_{0d}, m_{0s})$ is the quark current mass, which explicitly breaks the chiral symmetry of the Lagrangian, and g_s and g_t are coupling constants of the model and have dimensions of mass^{-2} and mass^{-5} , respectively.

The thermodynamic potential density Ω for a given baryonic chemical potential μ , at $T = 0$, is given by

$$\Omega = \mathcal{E} - \sum_i \mu_i \rho_i \quad (2)$$

where the sum is over the quark flavors ($i = u, d$ and s), μ_i and ρ_i are the chemical potential and the density, respectively, for each quark flavor i and

$$\mathcal{E} = -\eta N_c \sum_i \int_{k_{fi}}^{\Lambda_0} \frac{d^3 p}{(2\pi)^3} \frac{p^2 + m_{0i} M_i}{E_i} - 2g_s \sum_i \langle \bar{\psi} \psi \rangle_i^2 - 2g_t \langle \bar{u} u \rangle \langle \bar{d} d \rangle \langle \bar{s} s \rangle - \mathcal{E}_0, \quad (3)$$

is the energy density. Above, $k_{fi} = \theta(\mu_i - M_i) \sqrt{\mu_i^2 - M_i^2}$ is the Fermi momentum of the quark i , the constants $\eta = 2$ and $N_c = 3$ are the spin and color degeneracies, respectively, and the constant \mathcal{E}_0 is included to ensure that $\Omega = 0$ in the vacuum. The Λ_0 term is a regularization ultraviolet cutoff to avoid divergences in the medium integrals, and it is taken as a parameter of the model. The quark condensates and densities are defined, for each $i = u, d, s$, respectively, as

$$\phi_i = \langle \bar{\psi} \psi \rangle_i = -\eta N_c \int_{k_{fi}}^{\Lambda_0} \frac{p^2 dp}{2\pi^2} \frac{M_i}{E_i}, \quad (4)$$

where M_i is the constituent mass of the quark i and $E_i = \sqrt{p^2 + M_i^2}$, and

$$\rho_i = \langle \psi^\dagger \psi \rangle_i = \eta N_c \int_0^{k_{fi}} \frac{p^2 dp}{2\pi^2}. \quad (5)$$

Minimizing the thermodynamic potential with respect to the constituent quark mass M_i results in three gap equations,

$$M_i = m_{0i} - 4g_s \phi_i - 2g_t \phi_j \phi_k, \quad (6)$$

where $i = u, j = d$ and $k = s$ and cyclic permutations.

As shown by authors in [9, 11, 12] we calculate an effective dynamical bag pressure:

$$B_{eff} = B_0 - B, \quad (7)$$

where B is given by,

$$B = \eta N_c \sum_i \int_0^{\Lambda_0} \frac{p^2 dp}{(2\pi)^2} \left(\sqrt{p^2 + M_i^2} - \sqrt{p^2 + m_{0i}^2} \right) - 2g_s \sum_i \langle \bar{\psi} \psi \rangle_i^2 - 4g_t \langle \bar{u} u \rangle \langle \bar{d} d \rangle \langle \bar{s} s \rangle, \quad (8)$$

and $B_0 = B_{\rho_u=\rho_d=\rho_s=0}$ is a constant.

In this work we consider the following set of parameters [8, 21]: $\Lambda_0 = 631.4$ MeV, $g_s \Lambda^2 = 1.829$, $g_t \Lambda_0^5 = -9.4$, $m_{0u} = m_{0d} = 5.6$ MeV, and $m_{0s} = 135.6$ MeV. This set of parameters was chosen in order to fit the vacuum values for the pion mass, the pion decay constant, the kaon mass, the kaon decay constant and the quark condensates: $m_\pi = 139$ MeV, $f_\pi = 93.0$ MeV, $m_k = 495.7$ MeV, $f_k = 98.9$ MeV, $\phi_{vd} = \phi_{vu} = (-246.7 \text{ MeV})^3$, and $\phi_{vs} = (-266.9 \text{ MeV})^3$.

B. Chemical potential-dependent cutoff $\Lambda(\mu)$

As proposed by R. Casalbuoni *et al* in [18] and M. Baldo *et al* in [20], we will introduce a chemical potential dependency in the NJL model cutoff. This dependence implies that the vacuum constituent quark masses M_{vi} become chemical potential dependent and the same occurs to the coupling constants, g_s and g_t .

In order to obtain the renormalized coupling constants we consider that the values of the quark condensates in vacuum ϕ_{vi} are known properties of the model: $\phi_{vd} = \phi_{vu} = (-246.7 \text{ MeV})^3$, and $\phi_{vs} = (-266.9 \text{ MeV})^3$,

$$-\eta N_c \int_0^{\Lambda(\mu)} \frac{p^2 dp}{2\pi^2} \frac{M_i(\Lambda(\mu))}{E_i(\Lambda(\mu))} = \phi_{vi}. \quad (9)$$

The new constituent quark masses $M_{vi}(\Lambda(\mu))$ are solutions of these equations ($M_{vu} = M_{vd}$ because $\phi_{vu} = \phi_{vd}$) and the coupling constants are solutions of the two gap Eqs.(6)

$$\begin{aligned} M_{vu}(\Lambda(\mu)) &= m_{0u} - 4g_s(\Lambda(\mu))\phi_{vu} - 2g_t(\Lambda(\mu))\phi_{vd}\phi_{vs} \\ M_{vs}(\Lambda(\mu)) &= m_{0s} - 4g_s(\Lambda(\mu))\phi_{vs} - 2g_t(\Lambda(\mu))\phi_{vd}\phi_{vu}. \end{aligned}$$

at $\mu = 0$, for the constituent masses $M_{vi}(\Lambda(\mu))$ which satisfy Eq.(9).

In this paper we make two choices for the cutoff chemical potential dependency. We use the cutoff proposed in [20],

$$\Lambda_1 = \begin{cases} \Lambda_0, & \text{if } \mu \leq \mu_0 \\ \sqrt{9(\mu - \mu_0)^2 + \Lambda_0^2}, & \text{if } \mu > \mu_0 \end{cases} \quad (10)$$

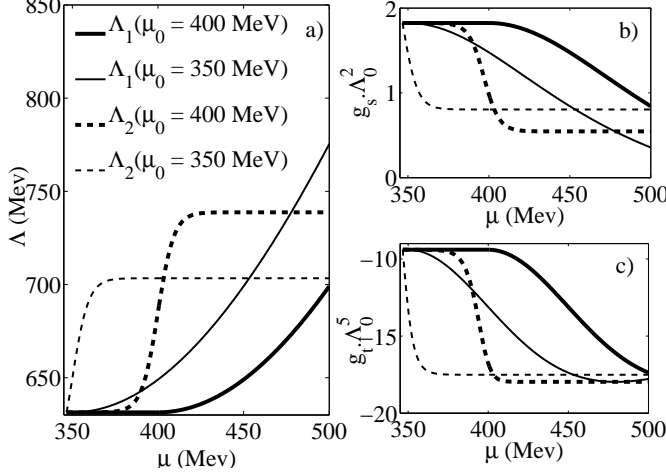


FIG. 1: Dependence on the chemical potential of a) the different parametrizations of the cutoffs discussed in the text; b) the g_s and c) g_t coupling constants.

where the term μ_0 is the value of chemical potential above which the cutoff becomes a function of the chemical potential. We also propose a new cutoff

$$\Lambda_2 = \Lambda_0 + a\Lambda_0 \left(\delta_0 - \frac{1}{1 + \exp\left(\frac{\mu - \mu_0}{b}\right)} \right), \quad (11)$$

where the constant a determines the maximum value of the cutoff and b how fast the cutoff increases with density. The constant δ_0 is given by

$$\delta_0 = \frac{1}{1 + \exp\left(\frac{\mu_c - \mu_0}{b}\right)}, \quad (12)$$

and ensures that $\Lambda_2(\mu_c) = \Lambda_0$. The constant μ_c is the chemical potential value for which the first drop of quark matter appears. P. Costa *et al* have calculated this parameter for each of the quarks: $\mu_u \simeq 312$ MeV $\mu_d = \mu_s \simeq 365$ MeV [22, 23] for the parameters chosen for this paper. We assume $\mu_c = 347$ MeV, approximately equal to $(\mu_d + \mu_u + \mu_s)/3$. In order to keep the vacuum properties the chemical potential dependence is introduced only for $\mu \geq \mu_c$. The parameter μ_0 determines the chemical potential range where the fastest increase of the cutoff occurs.

Λ_1 is one of the choices considered in [20] which was adjusted in order to keep the curve proposed in [18] with $\Lambda_0 \simeq 580$ MeV and $\mu_0 = 400$ MeV on a range of chemical potential between (400 – 600) MeV. In present work we are not concerned with keeping the curve proposed in [18], therefore we take different values for μ_0 (between 347 – 400 MeV for both cutoffs) in order to verify the effect of this parameter on the results obtained with the model. The cutoff Λ_2 of Eq.(11) is a particular choice where the numerical coefficients $a = 0.17$ and $b = 0.005$ are adjusted in order to obtain a fast increase to the cutoff on a small interval of the chemical potential and a

stabilization at some value (on the next sections we show the effect of the different values of the parameter a in our results). Fig. 1a) shows the plots of the two different cutoffs for two different values of μ_0 . For the cutoff Λ_2 the parameter μ_0 does not change the rate of growth of the cutoff, however it changes the region on the chemical potential range where the increase occurs. In the same figure we can see also the behavior of the coupling constants $g_s(\Lambda(\mu))$ [Fig. 1b)] and $g_t(\Lambda(\mu))$ [Fig. 1c)] as a function of the chemical potential. As discussed in [18, 20] the coupling constants decrease with the increase of cutoffs in both cases.

C. The thermodynamic consistency

The chemical dependent cutoff introduced in the $su(3)$ NJL model gives rise to some modifications in the thermodynamics of the system. The baryon thermodynamic potential is rewritten as

$$\Omega_b(k_f, \Lambda(\mu)) = \mathcal{E}(k_f, \Lambda(\mu)) - \sum_{i=u,d,s} \mu_i \rho_i + b(\Lambda, k_f), \quad (13)$$

where the term $b(\Lambda, k_f)$ is introduced in order to maintain thermodynamical consistency

$$\rho_i = -\frac{\partial \Omega}{\partial \mu_i}. \quad (14)$$

To calculate the the function b we use the prescription of Gorenstein and Yang [19] and we obtain:

$$b(\Lambda, k_f) = \frac{\eta N_c}{2\pi^2} \sum_{i=u,d,s} \int_{\Lambda_0}^{\Lambda} p^2 \sqrt{p^2 + M_i^2} dp + 2 \int_{\Lambda_0}^{\Lambda} \left(\sum_{i=u,d,s} \phi_i^2 \frac{\partial g_s}{\partial \Lambda} + \phi_u \phi_d \phi_s \frac{\partial g_t}{\partial \Lambda} \right) dp, \quad (15)$$

so that the condition $(\partial \Omega / \partial \Lambda)_{T, \mu} = 0$. In Fig. 2 we show that the thermodynamic condition defined in Eq.(14) is satisfied when we include the quantity $b(\Lambda, k_f)$ in the thermodynamic potential.

D. β -equilibrium condition

In the present section we build the equation of state (EOS) of strange quark stellar matter. We must impose both β -equilibrium and electric charge neutrality [1]. We will consider cold matter, after the neutrinos have diffused out and the neutrino chemical potential is zero. For β -equilibrium matter we add the lepton contribution to the thermodynamic potential,

$$\Omega(k_f, \Lambda(\mu)) = \Omega_b + \Omega_l, \quad (16)$$

where $\Omega_l = \mathcal{E}_l(k_{fl}) - \sum_l \mu_l \rho_l$ is the leptonic contribution taken as that of a free Fermi gas of electrons and muons.

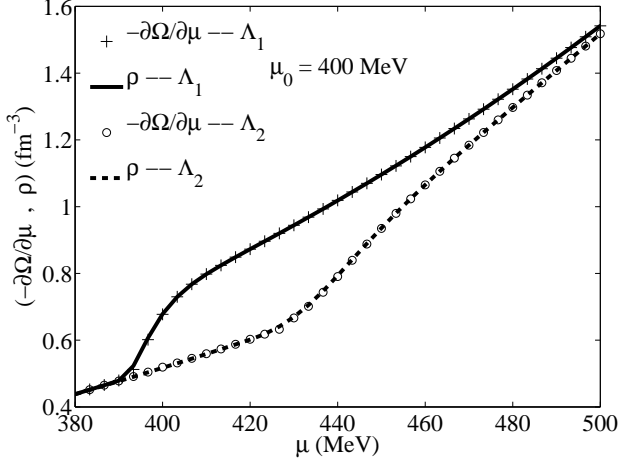


FIG. 2: Plot of the thermodynamic condition, Eq. (14), for the two parametrizations proposed (10,11).

The electron and muon densities are

$$\rho_l = \frac{1}{3\pi^2} k_{fl}^3. \quad (17)$$

In β -equilibrium the conditions of chemical equilibrium and charge neutrality are given by

$$\begin{aligned} \mu_s &= \mu_d = \mu_u + \mu_e, & \mu_e &= \mu_\mu, \\ \rho_e + \rho_\mu &= \frac{1}{3}(2\rho_u - \rho_d - \rho_s). \end{aligned} \quad (18)$$

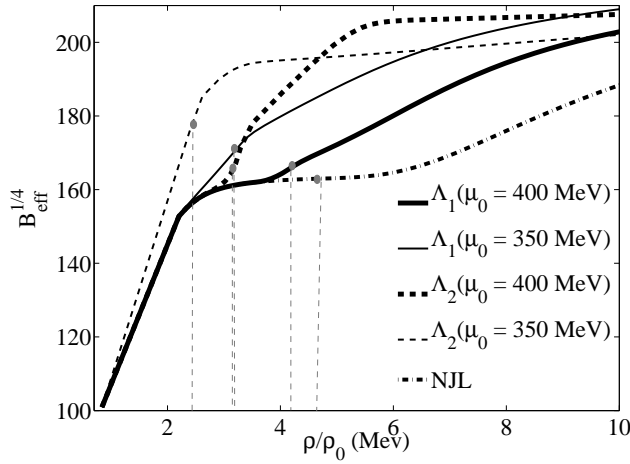


FIG. 3: Effective bag pressure defined in Eq. (7) for different parametrizations of the cutoff and stellar quark matter in β -equilibrium.

In Fig. 3 we plot the effective bag pressure, Eq.(8), for each choice of the cutoff and for quark matter in β -equilibrium as a function of the baryonic density $\rho_B = (\rho_u + \rho_d + \rho_s)/3$. As shown in references [11, 12] there is

a plateau around $B^{1/4} = 161 - 163$ MeV between $3\rho_0 - 5\rho_0$ in the standard NJL model. The plateau is due to the partial chiral symmetry restoration of quarks u and d . For the new parametrizations of the cutoff the value $B_{eff}^{1/4} \sim 162$ MeV will occur at lower densities and the plateau disappears in all cases. This effect occurs because the chemical potential dependence of the cutoff starts for a chemical potential below the partial chiral symmetry restoration for the quarks u and d . We have marked the onset of the strange quark on the effective bag curve with vertical lines. The effective bag stabilizes much faster for $\Lambda = \Lambda_2$ and tends to behave in a similar way to the MIT bag model with the decrease of the μ_0 .

In Fig. 4 we show the quark fractions, $Y_i = \rho_i/(3\rho_B)$ [Fig. 4a)], and the constituent masses of the u , d and s quarks in β -equilibrium [Fig. 4b)]. The effect of different choices of the cutoff on the quark s is clear: for the faster increase of $\Lambda(\mu)$ and smaller values of μ_0 the appearance of the quark s occurs at lower densities and the its constituent mass M_s approaches the current quark mass m_{0s} at lower densities too.

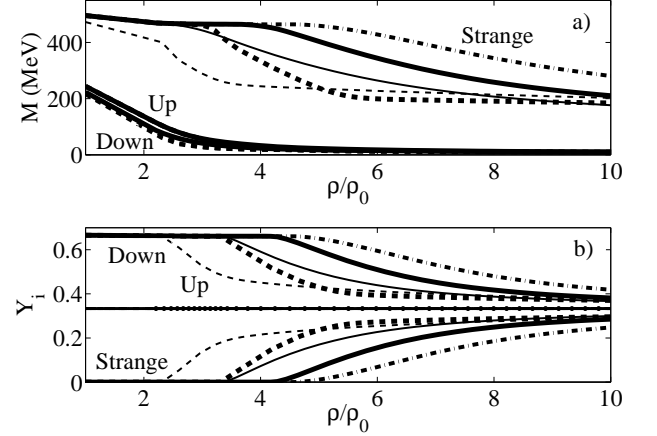


FIG. 4: Quark stellar matter in β -equilibrium with different choices of the cutoff: a) fractions and b) constituent masses of the quarks u , d , s as a function of density.

As can be seen from Figs. 3 and 4 the different slopes in the μ dependent cutoff and the different values of the chemical potential μ_0 change the behavior of the model, namely the constituent quark masses and baryonic density. The EOS becomes softer with these modifications, as seen in Fig. 5, where the pressure is displayed as a function of the chemical potential for the standard NJL model and the different choices of the cutoff. The cutoff dependence proposed in Eq. (11) gives the softest EOS. We also note that decreasing μ_0 favors a deconfinement phase transition at lower densities for both parametrizations of the cutoff, Λ_1 and Λ_2 . In the same figure we plot the EOS of the hadronic phase (dotted curve). The crossing point between the hadronic and the quark EOS indicates the phase transition from the hadronic phase to the quark phase using a Maxwell construction [24]. The

EOS of the quark phase constructed with standard NJL model does not cross the EOS of the hadronic phase on the chemical potential range shown.

The inclusion of a cutoff dependent on the chemical potential in the NJL model influences the deconfinement phase transition and, consequently, the stability of the star, as we will show in the next section.

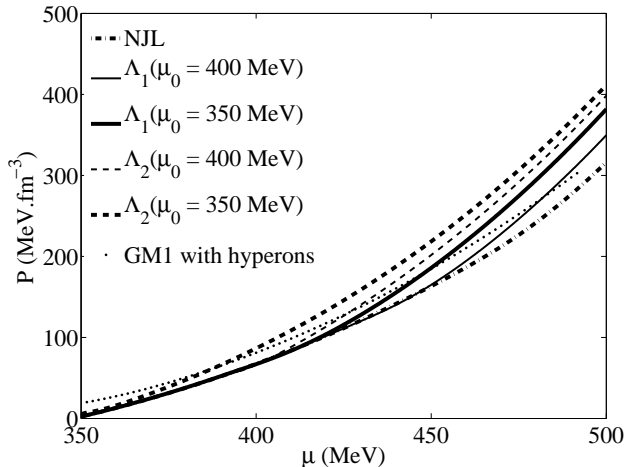


FIG. 5: Pressure as a function of the chemical potential for quark stellar matter in β -equilibrium with different choices of the cutoff and standard NJL model. The hadronic EOS, GM1 with hyperons [27], is also included (dotted curve).

III. THE NEUTRON STAR STABILITY

In this section we investigate the properties of stars constructed using the modified su(3) NJL model. The Maxwell construction [24] is considered for the phase transition from the hadronic phase to the quark phase. In this case the phase transition is identified by the crossing point between the hadronic and the quark EOS in the pressure versus baryonic chemical potential plane. At lower densities (below the transition point) an hadronic phase is favored and at higher densities (above the transition chemical potential) quark matter is favored.

However, we should point out that the Maxwell construction is an approximation for which only baryon number conservation is considered and does not take correctly into account the existence of two charge conserving conditions, nor surface effects and the Coulomb field [25, 26]. Instead, we could have considered a Gibbs construction [1], which takes into account the existence of two charge conserving conditions. However, a complete treatment of the mixed phase requires the knowledge of the surface tension between the two phases which is not well established and may have a value between 10-100 MeV/fm² [26]. The Gibbs construction gives results close to the ones obtained with the lower value of the above surface tension range, and is recovered for a zero surface tension,

while it has been shown in [26] that the Maxwell description of the mixed phase gives a good description if the surface tension is very large.

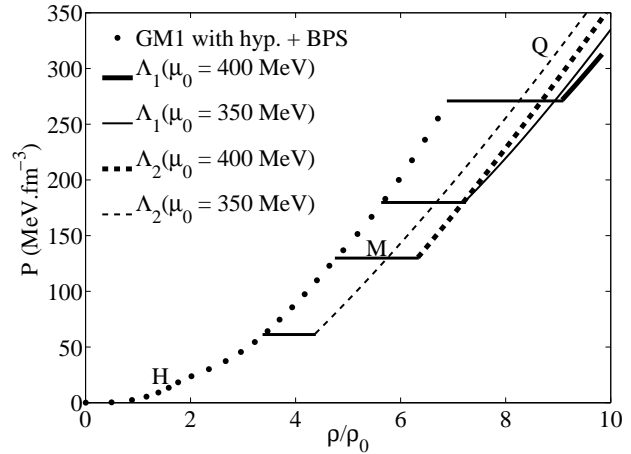


FIG. 6: EOS of hybrid stellar matter: Maxwell construction for a first order phase transition. Pressure as a function of the baryon density for different parametrizations of the cutoff. The hadronic, mixed and quark phases are identified respectively with a H, M and Q label.

For the hadronic sector we use a EOS proposed by Glendenning and Moszkowsky (GM1) [27] with the inclusion of the baryonic octet. In order to fix the hyperon coupling constants we have used one of choices discussed in literature [1, 27], namely we took for all the hyperons the same coupling constants which are a fraction x_i of the meson-nucleon coupling constants, $x_\sigma = 0.7$, $x_\omega = 0.783 = x_\rho$. For low densities (near zero density) we use the Baym, Pethick and Sutherland (BPS) model [28]. The standard and the modified su(3) NJL models are used to describe quark matter phase. In Fig. 6 we plot the pressure as a function of the baryonic density for the complete EOS discussed above. The plateaus, identified with an M, represent the deconfinement phase transition as a consequence of the first order Maxwell construction. In the case of cutoff Λ_1 and lower values of μ_0 the transition from hadron to quark phase occurs at lower values of the pressure and the plateau decreases. The same situation occurs with cutoff the Λ_2 .

The presence of strangeness in the core and crust of the star can have an important influence in the stability of the star [29, 30]. We have calculated the strangeness content of the EOS for the different parametrizations of the cutoff. In Fig. 7 we plot the strangeness fraction given by

$$r_s^{QS} = \frac{\rho_s}{3\rho},$$

for the quark phase and

$$r_s^{QS} = \frac{\sum_B |q_s^B| \rho_B}{3\rho},$$

for the hadronic phase. The term q_s^B is the strange charge baryon B .

The strangeness fraction is strongly modified by the different choices of the cutoff. As we can see in Fig. 7, in the case of Λ_1 with $\mu_0 = 400$ MeV, the strangeness fraction decreases in the mixed phase and increases again in the pure quark matter. However, with $\mu_0 = 350$ MeV the strangeness fraction increases in the mixed phase and continues to increase in the pure quark matter. For the case of Λ_2 the strangeness fraction increases in both cases in the mixed phase. These different behaviors are due to the densities at which the mixed phase occurs and the values of the constituent masses of the strange quark for these densities. The Table I shows the values of the constituent masses of strange quark on the mixed phase, the value of the densities at the onset of the phase transition, the width of the plateau of the mixed phase and the difference of the strangeness fraction between quark and hadronic phase.

TABLE I: Constituent masses of the strange quark, densities at the onset of the phase transition, width of the plateau of the mixed phases and difference of the strangeness fraction between quark and hadronic phase for each parametrization of the cutoff.

Cutoff	M_s (MeV)	ρ_{QP} (fm^{-3})	$\Delta\rho$ (fm^{-3})	Δr_s ($\times 10^{-2}$)
$\Lambda_1(\mu_0 = 400\text{MeV})$	229.16	1.00	0.32	-1.2
$\Lambda_1(\mu_0 = 350\text{MeV})$	225.23	0.82	0.23	2.9
$\Lambda_2(\mu_0 = 400\text{MeV})$	197.27	0.69	0.23	8.2
$\Lambda_2(\mu_0 = 350\text{MeV})$	240.61	0.49	0.14	10.1

The values of the density at the onset of the phase transition and the width of the plateau decrease when μ_0 decreases for both parametrizations of the cutoff. On the other hand, the discontinuity of the strangeness fraction between the two phases becomes positive and increases. The value of the constituent mass of the s quark generally decreases if μ_0 decreases except for Λ_2 with $\mu_0 = 350$ MeV that has the biggest constituent mass due to the low density at the phase transition density. According to references [11, 12] these results are directly relate with the possible existence of deconfined quark matter in the interior of neutron star as we will see later

We calculate the neutron star configuration for each cutoff solving the Tolman-Oppenheimer-Volkoff (TOV) equations for a spherically symmetric and static star[31, 32]. Fig. 8 shows the gravitational mass of hybrid stars of the maximum mass configuration as a function of (a) the radius and of (b) the central density for each cutoff. As we can see in these plots the maximum mass is influenced by the cutoff. In the Table II we show the values of the gravitational mass, central density and the radius of the maximum mass star configuration constructed with the EOS proposed in the present work as well as with the EOS proposed by Glendenning and Moszkowsky [1, 27].

The gravitational mass of the hybrid stars is characterized by a cusp in the mass versus radius plot and a

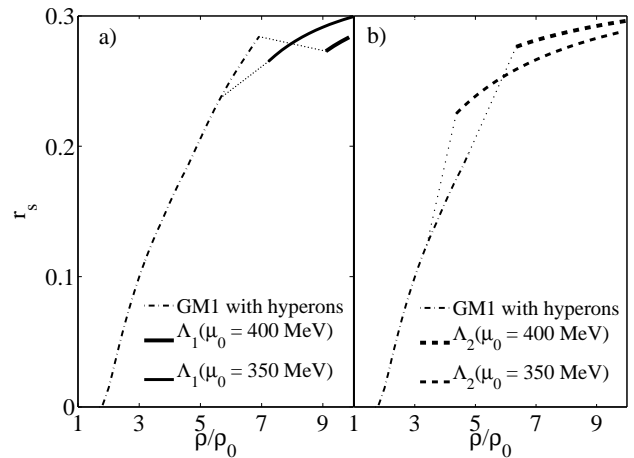


FIG. 7: Strangeness fraction r_s for different slopes of the cutoff for the quark phase: a) Λ_1 b) Λ_2 .

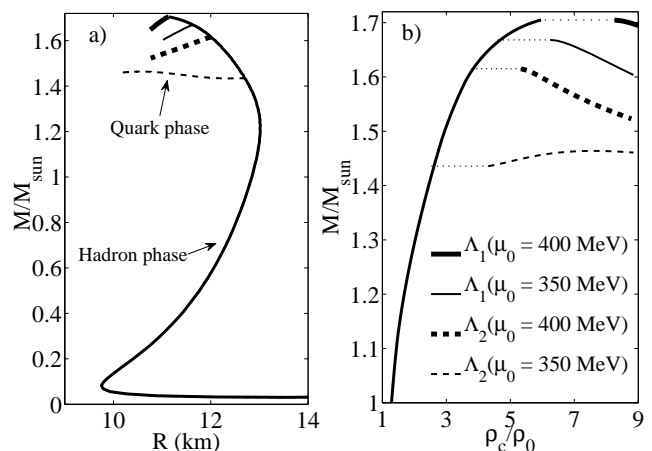


FIG. 8: The gravitational mass of the hybrid star is plotted as a function of a) the star radius and b) the central density, for the different parametrizations of the cutoff.

plateau in the mass versus central density graph. The plateau is a consequence of the Maxwell construction and corresponds to the mixed phase between a pure hadron and a pure quark phase. The cusp occurs at the onset of the quark phase in the interior of the star. We conclude that for most of the models the deconfinement phase transition makes the star unstable. However, for the cutoff Λ_2 with $\mu_0 = 350$ MeV the maximum mass configuration appears after the plateau and the cusp. In this case the star configuration with the maximum mass has a quark phase core. We verify that configurations with a quark phase core are possible only for the chemical potential $\mu_0 \lesssim 360$ MeV. For values of $\mu_0 \gtrsim 360$ MeV we have two possibilities: 1) instability of the hybrid star with the onset of a quark phase in the star as we can see in the case of $\mu_0 = 400$ MeV; 2) the EOS of hadronic phase is favored for all densities if $\mu_0 > 430$ MeV.

The μ_0 range with a stable quark core changes depending on the parameters used to Λ_2 . In Fig. (9) are shown the different configurations for the different values of μ_0 in the case of Λ_2 with $a = 0.17$. The value of maximum mass decreases if μ_0 increases. We have plotted the mass of the maximum mass configuration as a function μ_0 in Fig. 10. The limit of stability corresponds to the minimum in this plot. In Fig. 11 the different star configurations for different values of a and the same $\mu_0 = 347$ MeV, are shown. We conclude that increasing a decreases the mass of the maximum mass configuration and the corresponding radius, because the EOS becomes softer.

It is seen from Table II that a smaller parameter μ_0 and a harder cutoff Λ gives rise to a smaller maximum mass. The occurrence of a quark core reduces a lot the maximum mass but we can still get a reasonable value, $\sim 1.45 M_\odot$, which is consistent with the observed maximum neutron star masses, except for the still not confirmed, highly massive compact stars, the millisecond pulsars PSR B1516 + 02B [34], and PSR J1748-2021B [35] with masses well above $2 M_\odot$.

TABLE II: Maximum gravitational mass and radius of the hybrid stars (hs) and quark stars (qs) obtained with different parametrizations of the cutoff Λ and two values of the transition chemical potential μ_0 . In the last line the values for the maximum mass neutron star (ns) obtained with GM1 with hyperons [27]. M indicates inside the mixed phase.

Model/Cutoff	M_{max} (M_\odot)	R (km)	ϵ_i (fm^{-4})	ϵ_f (fm^{-4})	ϵ_c (fm^{-4})
$\Lambda_1(\mu_0 = 400\text{MeV})$	1.701	11.14	5.97	8.26	M
$\Lambda_1(\mu_0 = 350\text{MeV})$	1.674	11.64	4.69	6.22	M
$\Lambda_2(\mu_0 = 400\text{MeV})$	1.621	12.00	3.84	5.29	M
$\Lambda_2(\mu_0 = 350\text{MeV})$	1.456	10.56	2.60	3.42	7.62
GM1 with hyperons	1.705	11.11			5.99

Fig. 12 shows the u and s quark condensates as a function of the chemical potential for both cutoff parametrizations. For the cutoff Λ_1 the module of the condensates starts to increase for $\mu \gtrsim 475$ MeV. This is not the case Λ_2 : the module of the condensates decreases with density leading the system to chiral symmetry restauration. Therefore, the cutoff proposed in this work is physically favored to cutoff Λ_1 . We believe the behavior of Λ_1 at high densities is due to the high value of the cutoff Λ_1 at these densities.

IV. SUMMARY

We have studied the possibility of formation of stable compact stars with a quark core within the $\text{su}(3)$ NJL model with a chemical potential dependent ultra-violet cutoff. We use a $\text{su}(3)$ NJL model parametrization which describes the vacuum properties of low mass mesons (pions and kaons) and choose the parametrization of the cutoff so that it increases with density. One

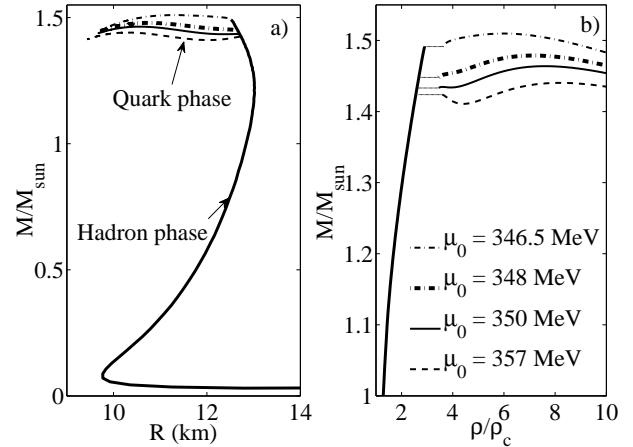


FIG. 9: The gravitational mass of the hybrid star is plotted as a function of a) the star radius and b) the central density, for different values of μ_0 for Λ_2 with $a = 0.17$.

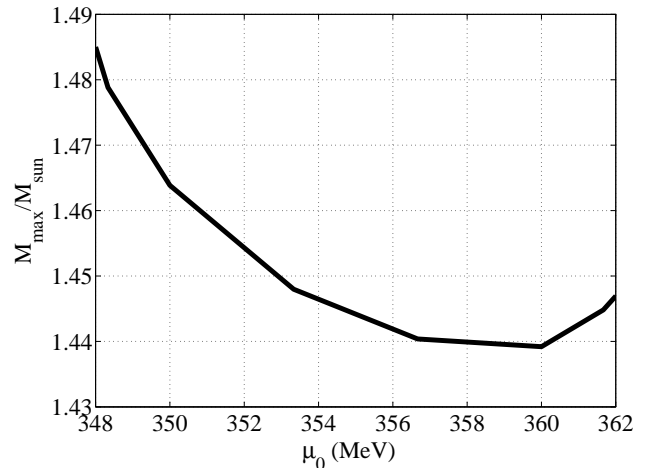


FIG. 10: Mass of the maximum mass star configuration as a function of the parameter μ_0 for Λ_2 with $a = 0.17$.

of the consequences of increasing the cutoff is a faster decrease the constituent s quark mass with density and, therefore, the onset of s quark at lower densities, giving rise to a larger pressure for the same chemical potential. The phase transition to a deconfined quark phase occurs at smaller densities and pressures and the density discontinuity at the phase transition is smaller. For cutoff Λ_2 ($a = 0.17$), stars with a quark core are obtained for a choice of the parameter $\mu_0 < 360$ MeV. The maximum mass of these stars is between $(1.46-1.51) M_\odot$, and is compatible with most of the compact star observations. However, the highly massive stars PSR B1516 + 02B [34], and PSR J1748-2021B [35], in case they are confirmed, would not reproduced.

According to Baldo *et al* the instability of compact stars within the NJL model is probably due to the lack

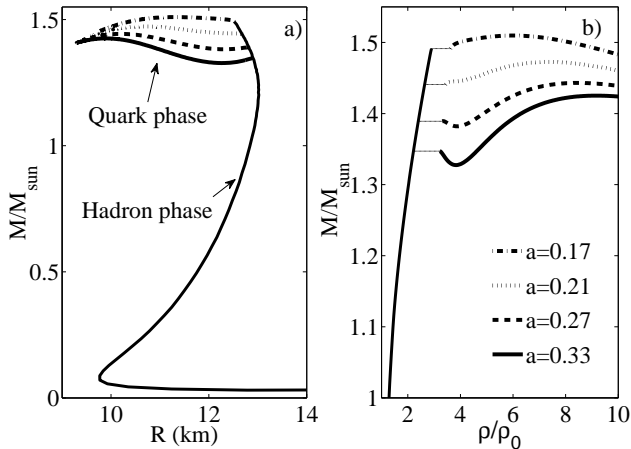


FIG. 11: The gravitational mass of the hybrid star is plotted as a function of a) the star radius and b) the central density, for different values of a for Λ_2 with $\mu_0 = 347$ MeV.

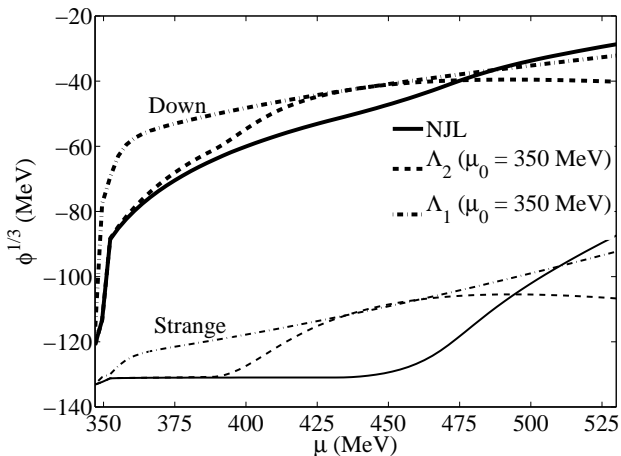


FIG. 12: Quark u and s condensates versus density for the different cutoff parametrizations.

of confinement in this model [20], since the authors of [36] were able to obtain stable stars with a quark core introducing a confining potential in the NJL model. The confining potential in the approach of [36] is switched off at the chiral phase transition. In [20] the authors have tried to get stable compact stars with a quark core using $su(2)$ NJL model with a cutoff dependent on the chemical potential and were not successful. Using the same dependence of the chemical potential, but introducing also the strange flavor we were also not able to obtain stable compact stars with a quark core. However, when we use the new cutoff proposed in this paper it is possible to get stable compact stars with a quark core if the strange flavor is included. We believe the stability of core quark occurs due to the fast increase of the cutoff Λ_2 allowing for a chiral symmetry restoration for the s -quark at much lower densities than the ones predicted by a constant cutoff. The result is an EOS soft enough to give rise to a quark core stable in a hybrid star. The stabilization of the cutoff at high densities is an important characteristic because it repares divergence problems due to the fast increase of the cutoff.

The effect of color superconductivity was not considered in the present work and will be the subject of a future work.

Acknowledgments

We would like to thank the fruitful discussions with João da Providência, Pedro Costa and Tobias Frederico. This work was partially supported by FEDER and Projects PTDC/FP/64707/2006 and CERN/FP/83505/2008, and by COMPSTAR, an ESF Research Networking Programme. CHL thanks to CAPES by the fellowship 2071/07-0 and the international cooperation program Capes-FCT between Brazil-Portugal.

-
- [1] N. K. Glendenning, *Compact Star* (Spring-verlag, New York, 2000).
 - [2] M. Prakash, I. Bombaci, M. Prakash, P. J. Ellis, J. M. Lattimer and R. Knorren, *Phys. Rep.* **280**, 1 (1997).
 - [3] A. Chodos, R.L. Jaffe, K. Johnson, C.B. Thorne and V.F. Weisskopf, *Phys. Rev. D* **9** (1974) 3471.
 - [4] C. Alcock, E. Farhi and A. Olinto, *Astrophys. J.* **310** (1986) 261.
 - [5] Y. Nambu and G. Jona-Lasinio, *Phys. Rev.* **122**, 345 (1961); **124**, 246 (1961).
 - [6] T. Hatsuda, T. Kunihiro, *Phys. Lett. B* **198**, 126 (1987); V. Bernard, R.L. Jaffe, U.-G. Meissner, *Nucl. Phys. B* **308**, 753 (1988). 753; M. Takizawa, K. Tsushima, Y. Kohyama, K. Kubodera, *Nucl. Phys. A* **507**, 611 (1990); S. Klimt, M. Lutz, U. Vogl, W. Weise, *Nucl. Phys. A* **516**, 429 (1990). 429; S.P. Klevansky, *Rev. Mod. Phys.* **64**, 649 (1992). 649; P. Rehberg, S.P. Klevansky, J. Hufner, *Phys. Rev. C* **53**, 410 (1996); M. Buballa, *Nucl. Phys. A* **611**, 393 (1996).
 - [7] T. Hatsuda and T. Kunihiro, *Phys. Rep.* **247**, 221 (1994).
 - [8] C. Ruivo, C. Sousa, and C. Providência, *Nucl. Phys. A* **651**, 59 (99).
 - [9] M. Buballa and M. Oertel, *Phys. Lett. B* **457**, 261 (1999).
 - [10] M. Buballa, *Phys. Rep.* **407**, 205 (2005).
 - [11] K. Schertler, S. Leupold, and J. Schaffner-Bielich, *Phys. Rev. C* **60**, 025801 (1999).
 - [12] D. P. Menezes and C. Providência, *Phys. Rev. C* **68**, 035804 (2003).
 - [13] D. P. Menezes and C. Providência, *Phys. Rev. C* **69**, 045801 (2004).
 - [14] D. Bailin and A. Love, *Phys. Rep.* **107**, 325 (1984); K. Rajagopal and F. Wilczek, *arXiv:hep-ph/0011333v2*; M.

- Alford, *Ann. Rev. Nucl. Part. Sci.* **51**, 131 (2001).
- [15] M. G. Alford, A. Schmitt, K. Rajagopal, T. Schafer, *Rev. Mod. Phys.* **80** (2008) 1455.
 - [16] R. Casalbuoni, G. Nardulli, *Rev. Mod. Phys.* **76** (2004) 263.
 - [17] L. McLerran, R. D. Pisarski, *Nucl. Phys. A* **796** (2007) 83; Y. Hidaka, L. McLerran, R. D. Pisarski, *Nucl. Phys. A* **808** (2008) 117; L. McLerran, K. Redlich, C. Sasaki, *Nucl. Phys. A* **824** (2009) 86.
 - [18] R. Casalbuoni, R. Gatto, G. Nardulli, and M. Ruggeri, *Phys. Rev. D* **68**, 034024 (2003).
 - [19] Mark I. Gorenstein and Shin Nan Yang, *Phys. Rev D* **52**, 5206 (1995).
 - [20] M. Baldo, G. F. Burgio, P. Castorina, S. Plumari, and Z. Zappal'a, *Phys. Rev. C* **75**, 035804 (2007).
 - [21] T. Kunihiro, *Phys. Lett. B* **219**, 363 (1989).
 - [22] P. Costa, M. C. Ruivo, and C. A. de Sousa, *Phys. Rev. D* **77**, 096001 (2008).
 - [23] P. Costa, M. C. Ruivo, C. A. de Sousa, and Y. L. Kalinovsky *Phys. Rev. C* **70**, 025204 (2004).
 - [24] Z. Fodor and S. D. Catz, *J. High Energy Phys.* **04**, 050 (2004).
 - [25] D. N. Voskresensky, M. Yasuhira, and T. Tatsumi, *Phys. Lett. B* **541**, 93 (2002); D. N. Voskresensky, M. Yasuhira, and T. Tatsumi, *Nucl. Phys. A* **723**, 291 (2003).
 - [26] T. Maruyama, S. Chiba, H-J Schulze, and T. Tatsumi, *Phys. Rev. D* **76**, 123015 (2007).
 - [27] N.K. Glendenning and S. Moszkowski, *Phys. Rev. Lett.* **67**, 2414 (1991).
 - [28] G. Baym, C. J. Pethick, and P. Sutherland, *ApJ* **170**, 299 (1971).
 - [29] C. Alcock, E. Farhi, and A. Olinto, *Astrophys. J.* **310**, 261 (1986).
 - [30] J.A. Pons, S. Reddy, M. Prakash, J.M. Lattimer, and J.A. Miralles, *Astrophys. J.* **513**, 780 (2001).
 - [31] R. C. Tolman, *Phys. Rev.* **55**, 364 (1939).
 - [32] J. R. Oppenheimer and G. M. Volkoff, *ibid.* **55**, 374 (1939).
 - [33] N. Itoh, *Prog. Theor. Phys.* **44**, **291** (1970); A.R. Bodmer, *Phys. Rev. D* **4**, 1601 (1971); E. Witten, *Phys. Rev. D* **30**, 272 (1984).
 - [34] Paulo C. C. Freire, Alex Wolszczan, Maureen van den Berg, and Jason W. T. Hessels, *Astrophys. J.* **679**, 1433 (2008).
 - [35] Paulo C. C. Freire, Scott M. Ransom, Steve Bégin, Ingrid H. Stairs, Jason W. T. Hessels, Lucille Frey, Fernando Camilo, *Astrophys. J.* **675**, 670 (2008).
 - [36] S. Lawley, W. Bentz, and A. W. Thomas, *J. Phys. G* **32**, 667 (2006).